ELSEVIER

Journal of Photochemistry and Photobiology A: Chemistry 148 (2002) 263–271

Journal of Photochemistry and Photobiology A:Chemistry

www.elsevier.com/locate/jphotochem

# Enhancing effects of water content and ultrasonic irradiation on the photocatalytic activity of nano-sized $TiO_2$ powders

Jimmy C. Yu [a,*], Jiaguo Yu [a,b], Lizhi Zhang [a], Wingkei Ho [a]

[a] *Department of Chemistry and Materials Science and Technology Research Center, The Chinese University of Hong Kong, Shatin, New Territories, Hong Kong*

[b] *State Key Laboratory of Advanced Technology for Materials Synthesis and Processing, Wuhan University of Technology, Wuhan 430070, China*

Received 24 July 2001; received in revised form 4 September 2001; accepted 4 September 2001

**Abstract**

A simple method for preparing highly photoactive nano-sized $TiO_2$ photocatalyst with anatase and brookite phase was developed by hydrolysis of titanium tetraisopropoxide in pure water or the EtOH/$H_2O$ mixed solution under ultrasonic irradiation. The prepared $TiO_2$ powders were characterized by differential thermal analysis (DTA), X-ray diffraction (XRD), X-ray photoelectron spectroscopy (XPS), transmission electron microscopy (TEM) and BET surface areas. The photocatalytic activity was evaluated by the photocatalytic oxidation of acetone in air. The results showed that the photocatalytic activity of $TiO_2$ powders prepared by this method from pure water or the EtOH/$H_2O$ mixed solutions with the molar ratio of EtOH/$H_2O$ = 1 exceeded that of Degussa P-25. The molar ratios of EtOH/$H_2O$ obviously influenced the crystallization, crystallite size, BET surface areas and photocatalytic activity of the prepared $TiO_2$ powders. Ultrasonic irradiation obviously enhanced the photocatalytic activity of $TiO_2$ powders whether the solvent is pure water or the EtOH/$H_2O$ mixed solutions. This may be ascribed to the fact that ultrasonic irradiation enhances hydrolysis of titanium alkoxide and crystallization of $TiO_2$ gel. 

*Keywords:* $TiO_2$ nano-sized powders; Sol–gel method; Ultrasonic; Water content; Photocatalytic activity

## 1. Introduction

A great deal of effort has been devoted in recent years to develop heterogeneous photocatalysts with high activities for environmental applications [1–4]. Among various oxide semiconductor photocatalysts, titania is a very important photocatalyst for its strong oxidizing power, nontoxicity and long-term photostability. Titania has three different crystalline phases: rutile, anatase and brookite, among which rutile is in thermodynamically stable state while the latter two phases are in metastable state [5]. Photocatalytic activity of titania may strongly depend on its phase structure, crystallite size, the specific surface areas and pore structure and so on, for example, many studies have confirmed that the anatase phase of titania is the superior photocatalytic materials for air purification, water disinfection, hazardous waste remediation, and water purification [1,2].

For the past two decades, the sol–gel routes have become an alternative method for the preparation of nanocrystalline materials [5,6]. It is known that the photocatalytic activity and phase transition behavior from amorphous to anatase phase are intensively influenced by the preparative conditions and methods [7–9]. Ito et al. [7] found that the volume ratio of $H_2O$/EtOH was a key factor influencing crystallinity and photocatalytic activity of $TiO_2$ particles prepared from the $H_2O$–EtOH mixed solution of $TiOSO_4$. However, to our knowledge, the effects of water content and ultrasonic irradiation on photocatalytic activity of nano-sized $TiO_2$ powders prepared by the sol–gel method have not been reported. Sonochemistry arises from acoustic cavitation, the formation, growth, and implosive collapse of bubbles in a liquid [10–12]. The collapse of bubbles generates localized hot spots with transient temperatures of about 5000 K, pressures of about 500 atm, and heating and cooling rates greater than $10^9$ K/s [10–12]. Therefore, the use of ultrasound to enhance the rate of reaction has become a routine synthetic technique for many homogeneous and heterogeneous chemical reactions [10–12].

In this study, a novel and simple method for preparing highly photoactive nano-sized $TiO_2$ photocatalyst with anatase and brookite phase has been developed by sol–gel method and ultrasonic treatment in pure water or the EtOH/$H_2O$ mixed solution. Enhancing effects and mechanisms of water content and ultrasonic irradiation on the photocatalytic activity of nano-sized $TiO_2$ powders were discussed.

* Corresponding author. Tel.: +852-26096268; fax: +852-26035057.
*E-mail address:* jimyu@cuhk.edu.hk (J.C. Yu).

1010-6030/02/$ – see front matter 
PII: S1010-6030(02)00052-7

## 2. Experimental

### 2.1. Preparation

All chemicals used in this study were reagent-grade supplied from Aldrich and were used as received. Millipore water was used in all experiments.

Titanium tetraisopropoxide (TTIP) was used as a titanium source. TTIP (0.0125 mol) was added dropwise to 100 ml pure water or EtOH/$H_2O$ mixed solution under vigorous stirring at room temperature. The molar ratio of EtOH/$H_2O$ ($R_{EtOH}$) was 0, 1, and 10, respectively. Sol samples obtained by the hydrolysis process were irradiated and unirradiated with ultrasonic in an ultrasonic cleaning bath (Bransonic ultrasonic cleaner, model 3210E DTH, 47 kHz, 120 W, USA) for 1 h, followed by aging in closed beaker at room temperature for 24 h in order to further hydrolyze the TTIP and obtain monodisperse $TiO_2$ particles. After aging, these samples were dried at 100 °C for about 8 h in air in order to vaporize water and alcohol in the gels and then ground to fine powders to obtain dry gel samples. The dried gel samples were calcined at temperatures 400, 500, 600 and 700 °C in air for 1 h, respectively.

### 2.2. Characterization

The X-ray diffraction (XRD) patterns obtained on a Philips MPD 18801 X-ray diffractometer using Cu Kα radiation at a scan rate of $2\theta = 0.05^\circ\,s^{-1}$ were used to determine the identity of any phase present and their crystallite size. The accelerating voltage and the applied current are 35 kV and 20 mA, respectively. The phase content of a sample can be calculated from the integrated intensities of anatase (1 0 1), rutile (1 1 0) and brookite (1 2 1) peaks. If a sample contains only anatase and rutile, the mass fraction of rutile ($W_R$) can be calculated from [13]

$$W_R = \frac{A_R}{0.886A_A + A_R} \tag{1}$$

where $A_A$ and $A_R$ represent the integrated intensity of the anatase (1 0 1) and rutile (1 1 0) peaks, respectively. If brookite is also present in a sample, similar relations can be derived [13]:

$$W_A = \frac{K_A A_A}{K_A A_A + A_R + K_B A_B} \tag{2a}$$

$$W_R = \frac{A_R}{K_A A_A + A_R + K_B A_B} \tag{2b}$$

$$W_B = \frac{K_B A_B}{K_A A_A + A_R + K_B A_B} \tag{2c}$$

where $W_A$ and $W_B$ represent the mass fraction of anatase and brookite, respectively, $A_B$ the integrated intensity of the brookite (1 2 1) peak, and $K_A$ and $K_B$ are the two coefficients and their values are 0.886 and 2.721, respectively. With Eqs. (2a)–(2c), the phase contents in any $TiO_2$ samples can be calculated. The average crystallite sizes of anatase, rutile, and brookite were determined according to the Scherrer equation using the FWHM data of each phase after correcting the instrumental broading [13].

The crystallization behavior is also monitored using a TG–DTA machine (model TG–DTA 92-16, Setaram, France). Crystallite sizes and shapes were observed using transmission electron microscopy (TEM) (Jcol, 1200EX, Japan). X-ray photoelectron spectroscopy (XPS) measurements were performed in the PHI Quantum 2000 XPS System with a monochromatic Al Kα source and a charge neutralizer; all the binding energies were referenced to the C 1s peak at 284.8 eV of the surface adventitious carbon. The Brunauer–Emmett–Teller (BET) surface area ($S_{BET}$) was determined using a Micromeritics ASAP 2000 nitrogen adsorption apparatus. All the samples measured were degassed at 180 °C before the actual measurements. The BET surface area and pore size distribution were directly given by the computer annexed to the apparatus.

### 2.3. Photocatalytic activity

Acetone ($CH_3COCH_3$) is a common chemical that is used extensively in a variety of industrial and domestic applications. For example, acetone is frequently used as a solvent in the printing industry and in analytical laboratories; it is a major constituent of many common household chemicals [14]. Therefore, we chose it as a model contaminate chemical. Photocatalytic oxidation of acetone is based on the following reaction [14,15]:

$$CH_3COCH_3 + 4O_2 \rightarrow 3CO_2 + 3H_2O \tag{3}$$

The photocatalytic activity experiments on $TiO_2$ powders for the oxidation of acetone in air were performed at ambient temperature using a 7000 ml reactor. The photocatalysts were prepared by coating an aqueous suspension of $TiO_2$ powders onto three dishes with diameters of 7.0 cm. The weight of the photocatalyst used for each experiment was kept at about 0.3 g. The $TiO_2$ photocatalysts were pretreated in an oven at 100 °C for about 2 h and then cooled to room temperature before use. After the dishes coated with $TiO_2$ powder photocatalysts were placed in the reactor, a small amount of acetone was injected into the reactor. The reactor was connected to a dryer containing $CaCl_2$ that was used for controlling the initial humidity in the reactor. The analysis of acetone, carbon dioxide, and water vapor concentration in the reactor was conducted with a Photoacoustic IR Multigas Monitor (INNOVA Air Tech Instruments Model 1312). The acetone vapor was allowed to reach adsorption equilibrium with the catalyst in the reactor prior to an experiment. The initial concentration of acetone after the adsorption equilibrium was about 400 ppm, which remained constant until a 15 W 365 nm UV lamp (Cole-Parmer Instrument) in the reactor was switched on. The initial concentration of water vapor was $1.20 \pm 0.01$ vol.%, and the initial temperature was $25 \pm 1$ °C. During the photocatalytic reaction, a near 3:1

ratio of carbon dioxide products to acetone destroyed was observed, and the acetone concentration decreased steadily with increase in UV illumination time. Each reaction was followed for 60 min.

The photocatalytic activity of the films can be quantitatively evaluated by comparing the apparent reaction rate constants. The photocatalytic degradation generally follows a Langmuir–Hinshelwood mechanism [1,2,16] with the rate $r$ being proportional to the coverage $\theta$:

$$r = k\theta = \frac{kKc}{1 + Kc} \tag{4}$$

where $k$ is the true rate constant which includes various parameters such as the mass of catalyst, the intensity of light, etc., and $K$ the adsorption constant. Since the initial concentration is low ($c_0 = 400\,\text{ppm} = 4.29 \times 10^{-3}\,\text{mol/l}$), the term $Kc$ in the denominator can be neglected with respect to unity and the rate becomes, apparently, first order:

$$r = -\frac{\mathrm{d}c}{\mathrm{d}t} = kKc = k_\mathrm{a}c \tag{5}$$

where $k_\mathrm{a}$ is the apparent rate constant of pseudo-first order. The integral form $c = f(t)$ of the rate equation is

$$\ln\frac{c_0}{c} = k_\mathrm{a}t \tag{6}$$

## 3. Results and discussion

### 3.1. Thermal analysis

Fig. 1 shows differential thermal analysis (DTA) curves of $TiO_2$ gel powders prepared from pure $H_2O$ (a) and EtOH/$H_2O$ mixed solutions ($R_{EtOH} = 10$) (b). It can be seen from Fig. 1(b) that a broad endothermic peak at below 150 °C and a relatively small exothermic peak at 266 °C are due to desorption of water and alcohol and decomposition of organic substances contained in the gel, respectively. At 373 °C, a very sharp exothermic peak is observed due to the formation of anatase phase [8,17]. Owing to the difference of the gel compositions, the positions and intensities of these peaks are obviously different in Fig. 1(a). Especially,

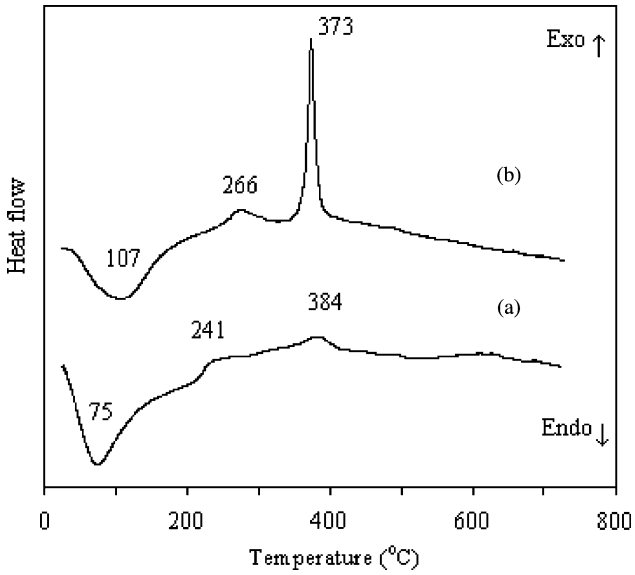


Fig. 1. DTA curves of $TiO_2$ gel powders prepared from the EtOH/$H_2O$ mixed solutions under ultrasonic irradiation with: (a) $R_{EtOH} = 0$ (pure water); (b) $R_{EtOH} = 10$ and dried at 100 °C for 8 h.

the exothermic peak intensity of formation of anatase phase in Fig. 1(a) is much smaller than that in (b). This is assigned to the former mostly transformed into anatase phase at low temperature (as shown in Table 1). Usually, the concentration of alkyl (OR) groups in the network structure decreases as the amount of water is increased in the hydrolysis medium. However, in the titania system, it was found that a certain concentration of OR groups always remains in the structure, regardless of the amount of water present [9]. Therefore, the exothermic peak at 241 °C in Fig. 1(a) is due to decomposition of residual unhydrolyzed alkyls in $TiO_2$ gel samples prepared from pure water, but the relative intensity of peaks decreased owing to the decrease in the amount of the unhydrolyzed residual alkyls.

### 3.2. Crystal structure

Table 1 shows XRD results of the as-prepared $TiO_2$ gel powders from the EtOH/$H_2O$ mixed solutions ($R_{EtOH} = 0$,

Table 1
Effects of calcination temperature and $R_{EtOH}$ on phase structure, phase content and average crystalline size of $TiO_2$[a,b]

| $R_{EtOH}$ | 100 °C for 8 h | 400 °C for 1 h | 500 °C for 1 h | 600 °C for 1 h | 700 °C for 1 h |
|---|---|---|---|---|---|
| 0 | A: 5.2 (69.5)<br>B: 5.3 (30.5) | A: 7.9 (75.1)<br>B: 7.4 (24.9) | A: 9.5 (79.6)<br>B: 7.9 (20.4) | A: 19.2 (69.5)<br>B: 13.1 (6.9)<br>R: 25.6 (2.6) | A: 33.6 (15.0)<br>R: 46.2 (85.0) |
| 1 | A: 3 | A: 8.3 (86.1)<br>B: 7.7 (13.9) | A: 11.3 (91.6)<br>B: 8.2 (9.4) | A: 27.3 (98.0)<br>R: 25.1 (2.0) | A: 40.2 (41.1)<br>R: 57.3 (58.9) |
| 10 | Am | A: 22.1 | A: 25.8 | A: 28.3 | A: 48.8 (79.8)<br>R: 77.0 (20.2) |

[a] A, B, R and Am denote anatase, brookite, rutile and amorphous, respectively.
[b] Average crystalline size of $TiO_2$ was determined by XRD using Scherrer equation.

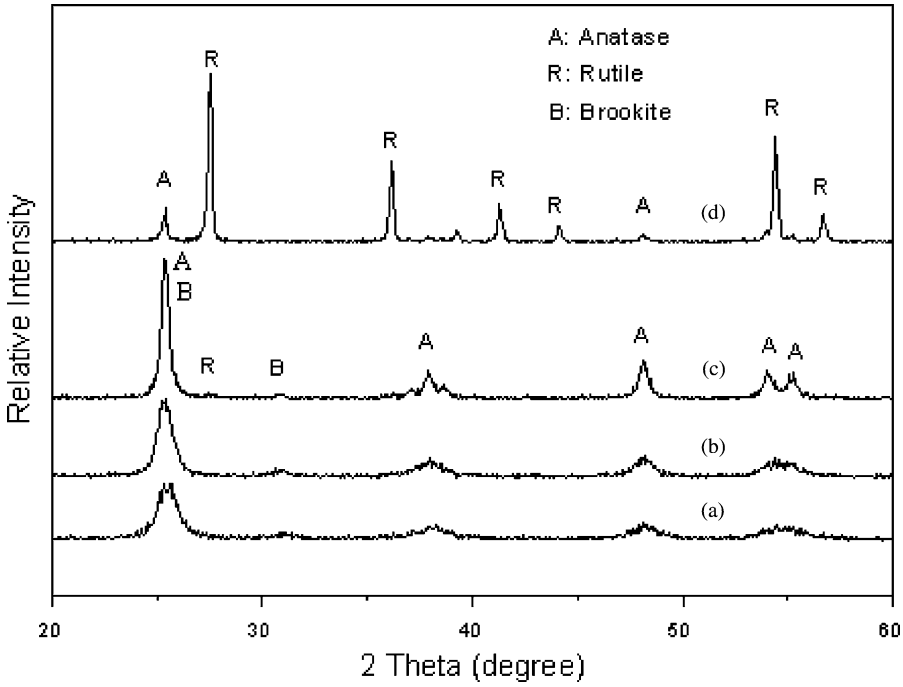


Fig. 2. XRD patterns of $TiO_2$ powders prepared from pure water under ultrasonic irradiation and calcinations at: (a) 400 °C; (b) 500 °C; (c) 600 °C; (d) 700 °C for 1 h.

1 and 10) after dried at 100 °C for 8 h. The $TiO_2$ gel powders obtained from pure water ($R_{EtOH} = 0$) contain anatase, as main phase, and brookite phase. With increasing $R_{EtOH}$, the intensities of anatase peaks steadily become weak and meanwhile brookite phase disappears. When $R_{EtOH} = 10$, the $TiO_2$ gel powders completely appear amorphous. This is probably due to the fact that EtOH solvent suppresses the hydrolysis of titanium alkoxide and rapid crystallization of the $TiO_2$ particles by adsorbing on the surfaces of $TiO_2$ particles [7]. Usually, with increasing water content, a stronger nucleophilic reaction between $H_2O$ and alkoxide molecules will occur and more alkoxyl groups in the alkoxide will be substituted by hydroxyl groups of $H_2O$ [18]. Therefore, the decrease of the quantity of unhydrolyzed alkyls in precursors results in reduction in steric hindrance by the residual alkyls preventing crystallization to crystalline anatase [8]. Fig. 2 shows XRD patterns of $TiO_2$ powders prepared from pure water, after calcinations at: (a) 400 °C; (b) 500 °C; (c) 600 °C and (d) 700 °C for 1 h. Fig. 2 shows that with increasing calcination temperature (from 400 to 600 °C), the peak intensities of anatase increase and the width of the (1 0 1) plane diffraction peak of anatase ($2\theta = 25.4°$) becomes narrower. At 600 °C, rutile phase appears, $TiO_2$ powders meanwhile contain three different phases: anatase, brookite and rutile. At 700 °C, rutile is a main phase and brookite disappears. Table 1 also shows the phase content and average crystalline size of $TiO_2$ samples as a function of calcination temperature and $R_{EtOH}$. It can be seen from Table 1 that when $R_{EtOH} = 0$, with increasing calcination temperature, the average crystallite size of anatase increases, the content of brookite decreases and finally disappears at 700 °C. Fig. 3 shows XRD patterns of $TiO_2$ powders prepared from the EtOH/$H_2O$ mixed solutions ($R_{EtOH} = 10$) after calcinations at: (a) 400 °C; (b) 500 °C; (c) 600 °C and (d) 700 °C for 1 h. $TiO_2$ powders only contain anatase phase at 400 °C and rutile phase appears at 700 °C. Table 1 shows not only that the average crystallite size of $TiO_2$ powders prepared from the EtOH/$H_2O$ solutions ($R_{EtOH} = 10$) is obviously larger than that of $TiO_2$ powders prepared from pure water, but also the content of rutile at 700 °C decreases with increasing $R_{EtOH}$. The former is ascribed to the phase transformation of amorphous to anatase occurred at about 373 °C causing the growth of anatase crystallites by providing the heat of transformation. The latter is due to the increase of steric hindrance caused by the residual unhydrolyzed alkyls.

Fig. 4 shows TEM photographs of $TiO_2$ powders prepared by hydrolysis of TTIP in pure water under ultrasonic irradiation and calcined at: (a) 500 °C and (b) 700 °C for 1 h. At 500 °C, the size of the primary particle is about $10 \pm 2$ nm, which is in agreement with the value determined from XRD analyses (9.5 nm). At 700 °C, some of the particles are fused together through sintering, which explains the significant decrease in $S_{BET}$ with increasing calcining temperature.

### 3.3. BET surface areas and pore structure

Fig. 5 shows the effects of calcining temperature and $R_{EtOH}$ on BET surface areas of $TiO_2$ powders. The as-prepared $TiO_2$ gel powders from pure water dried at 100 °C show a very large $S_{BET}$ value of 219.9 $m^2\,g^{-1}$. The

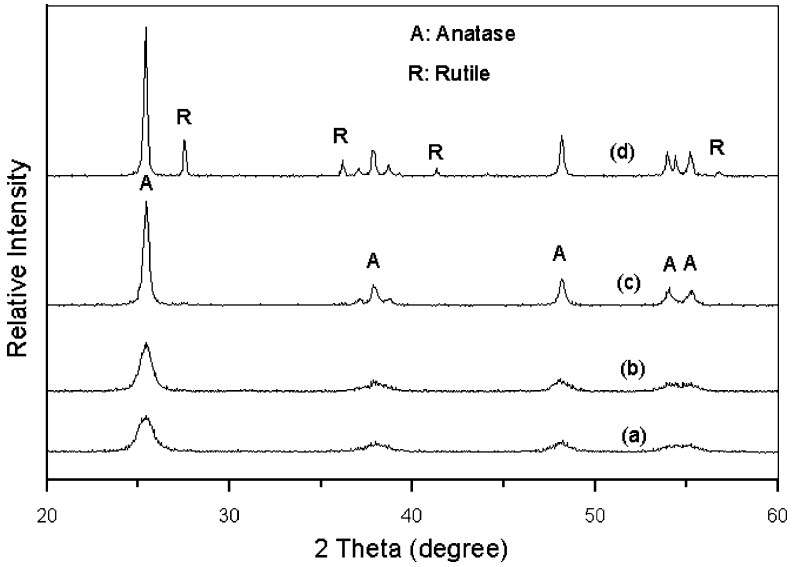


Fig. 3. XRD patterns of $TiO_2$ powders prepared from the EtOH/$H_2O$ solutions ($R_{EtOH} = 10$) under ultrasonic irradiation and calcinations at: (a) 400 °C; (b) 500 °C; (c) 600 °C; (d) 700 °C for 1 h.

values decrease monotonically with an increase in calcination temperature. This is due to the increase in average crystallite size of $TiO_2$ powders (as shown in Table 1). Owing to sintering and phase transformation of anatase to rutile, at 700 °C, the BET surface area of the same sample decreased drastically to 2.04 $m^2 g^{-1}$. When $R_{EtOH} = 1$, the $S_{BET}$ value of $TiO_2$ at 100 °C is higher than that of $TiO_2$ prepared from pure water ($R_{EtOH} = 0$) at 100 °C. This is due to the former with smaller $TiO_2$ crystallite (3 nm). When calcining temperature is over 400 °C, the $S_{BET}$ value of $TiO_2$ prepared from pure water ($R_{EtOH} = 0$) is larger than that of $TiO_2$ prepared from the EtOH/$H_2O$ mixed solution ($R_{EtOH} = 1$ or 10). This may be ascribed to the fact that the more the amount of water in hydrolysis medium, the faster the speed of hydrolysis and polycondensation of ≡Ti–OR and ≡Ti–OH species, the more the seed nuclei, the smaller $TiO_2$ crystallites.

Fig. 6 shows pore size distribution curve calculated from the desorption branch of the nitrogen isotherm by the Barrett–Joyner–Halenda (BJH) method and the corresponding nitrogen adsorption–desorption isotherms (inset) of $TiO_2$ powders prepared from the EtOH/$H_2O$ solution ($R_{EtOH} = 10$) and calcined at 500 °C for 1 h. The sharp decline in the desorption curve is indicative of mesoporosity, while the hysteresis between the two curves demonstrates that there is a diffusion bottleneck, possibly caused by non-uniform pore size. The pore size distribution calculated from the desorption branch of the nitrogen isotherm by the BJH method showed that average pore diameter is ca. 7.2 nm and the range of pores is narrow (2.5–12.5 nm).

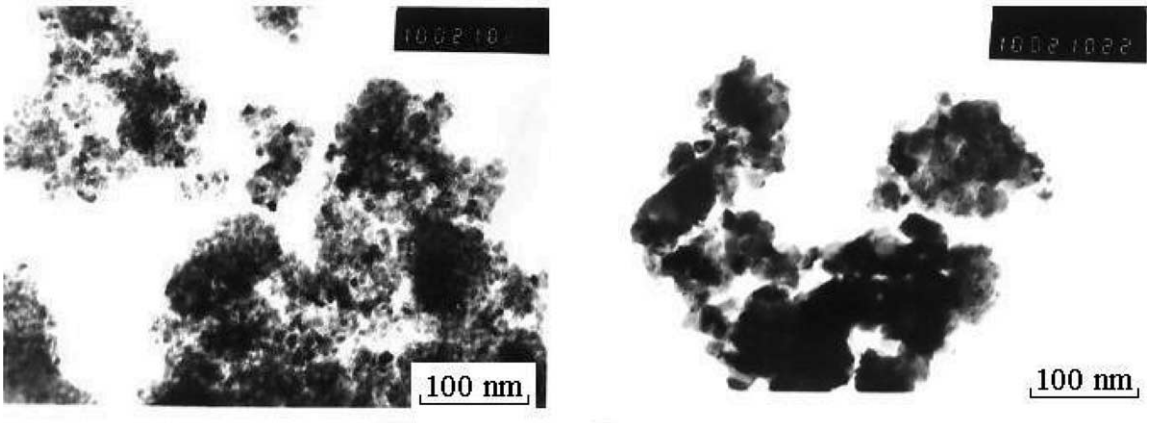


Fig. 4. TEM photographs of $TiO_2$ powders prepared by hydrolysis of TTIP in pure water under ultrasonic irradiation and calcination at: (a) 500 °C; (b) 700 °C for 1 h.

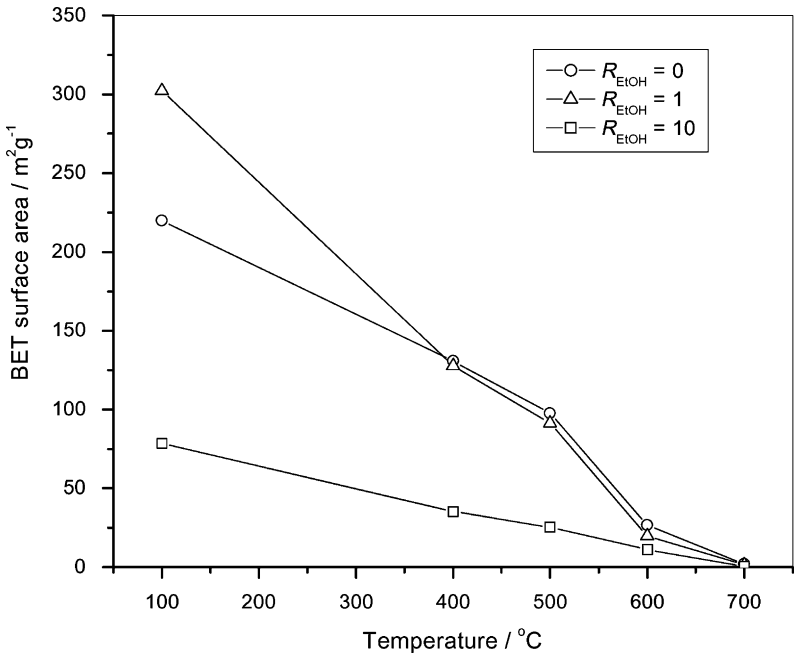


Fig. 5. The effects of calcination temperature and $R_{EtOH}$ on BET surface areas of $TiO_2$ powders.

The BET surface areas and pore parameters of the samples determined from nitrogen adsorption–desorption isotherm by the BJH method are summarized in Table 2. The table shows all other samples calcined at 500 °C with mesoporous structure, also their pore size distribution curve and nitrogen adsorption and desorption isotherms are similar to those of $TiO_2$ powders prepared from the $EtOH/H_2O$ solution ($R_{EtOH} = 10$) and calcined at 500 °C for 1 h (not shown here). The average pore diameters were also several nanometers. The mesoporous structure of $TiO_2$ particles is attributed to pores formed between $TiO_2$ particles [19]. It is these mesoporous pores that allow rapid diffusion of various reactants and products during photocatalytic reaction and enhance the speed of photocatalytic reaction. It can also be seen from Table 2 that with increasing $R_{EtOH}$, BET surface area, porosity and pore volume decrease and pore diameter

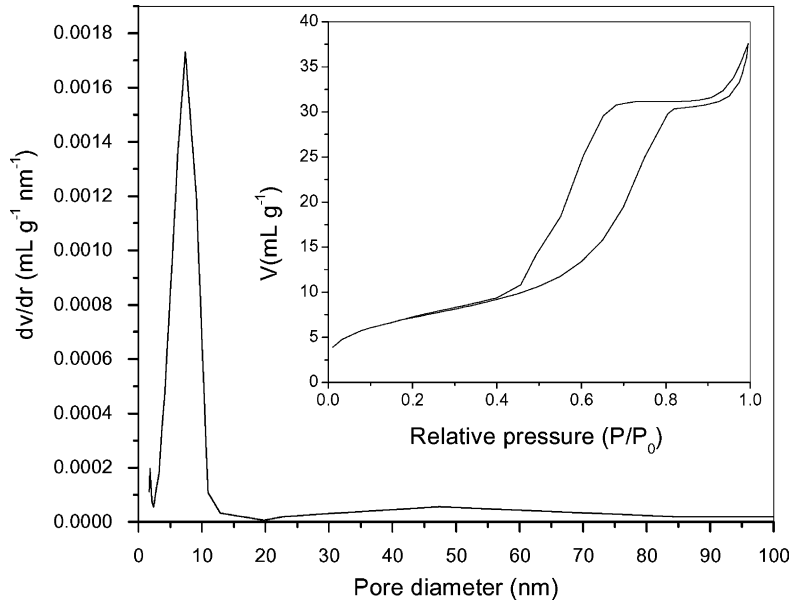


Fig. 6. Pore size distribution curve calculated from the desorption branch of the nitrogen isotherm by the BJH method. Inset: the corresponding nitrogen adsorption–desorption isotherms of nano-sized $TiO_2$ powders prepared from the $EtOH/H_2O$ solution ($R_{EtOH} = 10$) under ultrasonic irradiation and calcined at 500 °C for 1 h.

Table 2
The effect of ultrasonic irradiation on BET surface areas and pore parameters of $TiO_2$ powders calcined at 500 °C

| $R_{EtOH}$[a] | Ultrasonic irradiation | $S_{BET}$ ($m^2\,g^{-1}$)[b] | Porosity[c] | Pore volume ($ml\,g^{-1}$)[d] | Pore size (nm)[e] |
|---|---|---|---|---|---|
| 0 | Yes | 97.61 | 50.6 | 0.218 | 5.9 |
| 1 | Yes | 91.38 | 48.1 | 0.192 | 5.3 |
| 10 | Yes | 26.34 | 17.7 | 0.052 | 7.2 |
| 0 | No | 75.51 | 42.7 | 0.188 | 7.1 |
| 1 | No | 67.5 | 36.3 | 0.136 | 6.8 |
| 10 | No | 22.3 | 9.8 | 0.029 | 6.5 |

[a] The molar ratios of $EtOH/H_2O$.
[b] BET surface area calculated from the linear part of the BET plot ($P/P_0 = 0.05$–$0.3$).
[c] The porosity is estimated from the pore volume determined using the adsorption branch of the $N_2$ isotherm curve at the $P/P_0 = 0.995$ single point.
[d] Total pore volume, taken from the volume of $N_2$ adsorbed at $P/P_0 = 0.995$.
[e] Average pore diameter, estimated using the adsorption branch of the isotherm and the BJH formula.

increases, which is attributed to the growth of $TiO_2$ crystallites. These result in the reduction in photocatalytic activity of $TiO_2$ particles (as shown in Fig. 8).

### 3.4. XPS analysis for composition

A common concern is whether residual carbon caused by carbonization of organic groups can be completely removed from the powders during heat treatment. To identify the composition of the samples, XPS analyses were carried out. Fig. 7 shows the wide-scan XPS spectrum of $TiO_2$ powders prepared from pure water and calcination at 500 °C. It shows that $TiO_2$ powders contain only Ti, O and C elements. The photoelectron peak for Ti 2p appears clearly at a binding energy, $E_b = 458.2$ eV, O 1s at $E_b = 531.2$ eV and C 1s at $E_b = 284.6$ eV. All of the binding energies at various peaks were calibrated using the binding energy of C 1s (284.8 eV). The atomic ratio of Ti to O is 1:2.03, as expected. In order to determine whether C element is the residual carbon from precursor solution or the adventitious hydrocarbon from XPS instrument itself, the surface of the powder sample was bombarded by a 5 keV $Ar^+$ beam to remove the contamination on the specimen. The wide-scan XPS spectrum of the specimen after $Ar^+$ sputtering for 5 min showed that C 1s peak disappeared. The results suggest that carbon on the surface of the powders is probably due to contamination caused by specimen handing or pumping oil. On the other hand, if the atomic percentage of residual carbon from precursor solution was more than 0.1% in the powder, another weak C 1s peak should have been observed at 288.6 eV. Such a peak, however, was not detected in the narrow-scan XPS spectrum of the C 1s peak of the

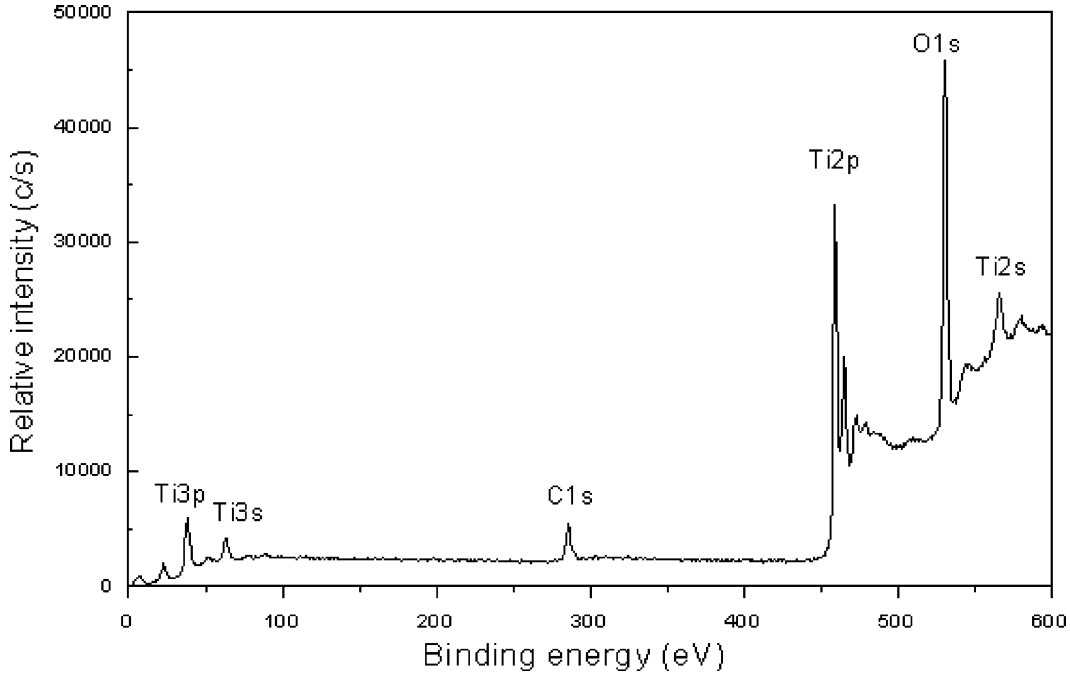


Fig. 7. XPS survey spectrum of nano-sized $TiO_2$ powders prepared by hydrolysis of TTIP in pure water under ultrasonic irradiation and calcination at 500 °C for 1 h.

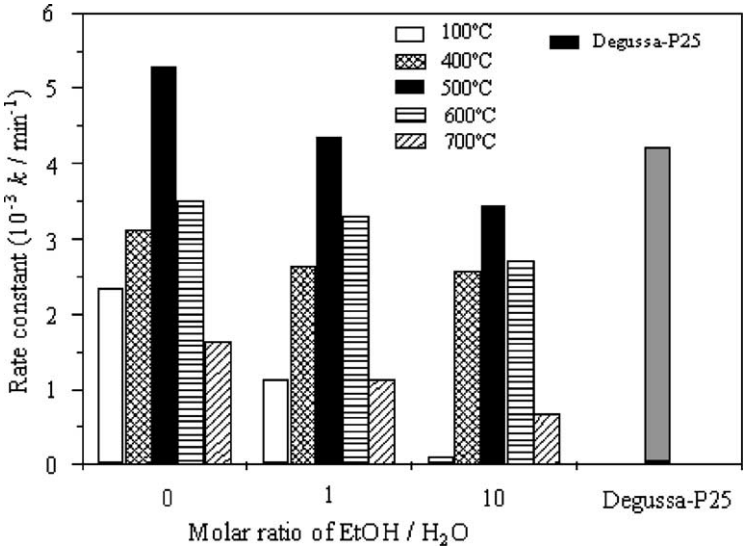


Fig. 8. The dependence of the apparent rate constants ($k$, min$^{-1}$) on calcination temperature and $R_{EtOH}$, all the samples were prepared by ultrasonic irradiation.

as-prepared powders. The C 1s peak at 284.6 eV is symmetric and narrow, indicating further that carbon on the surface of the powders is due to the contamination.

### 3.5. Photocatalytic activity

Fig. 8 shows the dependence of the apparent rate constants ($k$, min$^{-1}$) on calcination temperature and the molar ratios of EtOH/$H_2O$ ($R_{EtOH}$). For $TiO_2$ powder prepared from pure water under ultrasonic irradiation and dried at 100 °C, it showed a good photocatalytic activity. Its $k$ reached $2.34 \times 10^{-3}$. This is assigned to formation of anatase at 100 °C and high specific surface areas. With increasing calcination temperature, the $k$ obviously increased. At 500 °C, the $k$ reached the highest value and its value was $5.30 \times 10^{-3}$. The $k$ was determined to be $4.19 \times 10^{-3}$ for Degussa P-25 (P25), which is well known to have a high photocatalytic activity [1,20]. The photocatalytic activity of $TiO_2$ powder prepared from pure water at 500 °C exceeded that of P25, which may be attributed to the fact that the former had larger specific

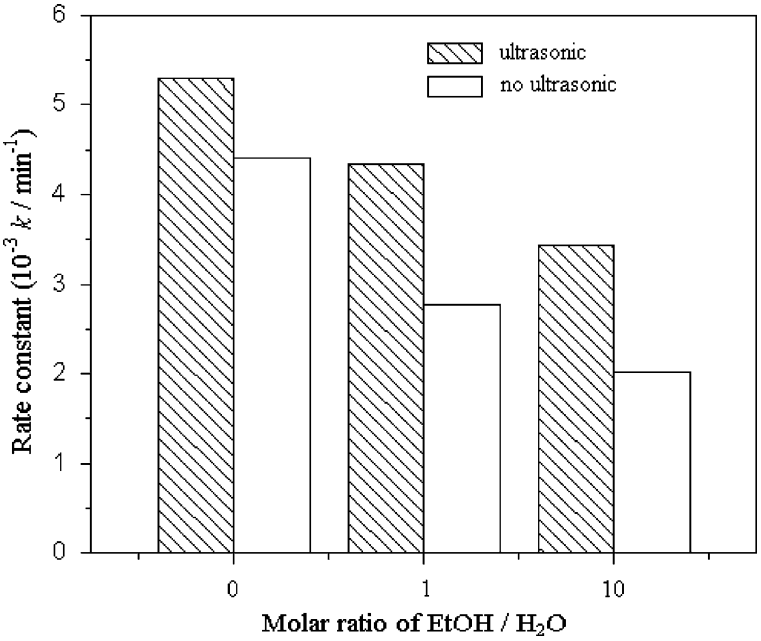


Fig. 9. The effect of ultrasonic irradiation on photocatalytic activity of nano-sized $TiO_2$ powders prepared from the EtOH/$H_2O$ solutions with $R_{EtOH} = 0$ (pure water), 1 and 10.

surface areas, smaller crystallite size and higher purity, etc. Usually, the specific surface areas and crystallite size of P25 are about $50\,m^2\,g^{-1}$ and 30 nm, respectively. Our XPS results showed that P25 contains a small amount of Cl element (about 0.5 atom%). With further increasing calcining temperature, the $k$ significantly decreased. This is due to the phase transformation of anatase to rutile, crystalline growth and drastic decrease in specific surface areas.

It can also be seen from Fig. 8 that with an increase in $R_{EtOH}$, the $k$ decreases at the same temperature. For example, for $TiO_2$ powders prepared from the EtOH/$H_2O$ solutions with $R_{EtOH} = 10$, at 100 °C, it showed almost no photocatalytic activity (negligible). This is due to $TiO_2$ being in amorphous status. At 500 °C, its $k$ is also lower than that of P25 and $TiO_2$ powder prepared from pure water or the EtOH/$H_2O$ solutions with $R_{EtOH} = 1$. This is attributed to the fact that it had smaller specific surface area and larger crystallite size. On the other hand, P25 and $TiO_2$ powder prepared from pure water or the EtOH/$H_2O$ solutions with $R_{EtOH} = 1$ all are composed of two phases, corresponding to anatase and rutile and anatase and brookite, respectively. Usually, the composite of two kinds of semiconductors or two phases of the same semiconductor is beneficial to reduce the combination of photo-generated electrons and holes and enhance photocatalytic activity.

Fig. 9 shows the effect of ultrasonic treatment on photocatalytic activity [21]. It can be seen from Fig. 9 that ultrasonic treatment obviously enhance the photocatalytic activity of $TiO_2$ powders whether the solvent is pure water or the EtOH/$H_2O$ mixed solutions. This may be ascribed to the fact that ultrasonic irradiation enhance hydrolysis of titanium alkoxide and crystallization of $TiO_2$ gel, because ultrasonic cavitation creates a unique environment for hydrolysis of titanium alkoxide.

## 4. Conclusions

The photoactive nano-sized (about 5 nm) $TiO_2$ powders with both anatase and brookite phases were synthesized at 100 °C from pure water by sol–gel method under ultrasonic irradiation. At 500 °C, the photocatalytic activity of $TiO_2$ powders prepared by this method from pure water or the EtOH/$H_2O$ mixed solutions with the molar ratio of EtOH/$H_2O$ = 1 showed very high photocatalytic activity and exceeded that of Degussa P-25. The molar ratios of EtOH/$H_2O$ greatly influenced the crystallinity, crystallite size, BET surface areas and photocatalytic activity of the prepared $TiO_2$ powders. Ultrasonic irradiation obviously enhances the photocatalytic activity of $TiO_2$ powders whether the solvent is pure water or the EtOH/$H_2O$ mixed solutions. This may be ascribed to the fact that ultrasonic irradiation enhances hydrolysis of titanium alkoxide and crystallization of $TiO_2$ gel.

## Acknowledgements

This work was partially supported by a grant from the National Natural Science Foundation of China and Research Grants Council of the Hong Kong Special Administrative Region, China (Project No. N_CUHK433/00). This work was also financially supported by the Foundation for University Key Teachers of the Ministry of Education and the National Natural Science Foundation of China (50072016).

## References

[1] M.R. Hoffmann, S.T. Martin, W. Choi, D.W. Bahnemann, Chem. Rev. 95 (1995) 69.
[2] A. Fujishima, T.N. Rao, D.A. Tryk, J. Photochem. Photobiol. C 1 (2000) 1.
[3] A.L. Linsebigler, G. Lu, J.T. Yates Jr., Chem. Rev. 95 (1995) 735.
[4] H. Tada, M. Yamamoto, S. Ito, Langmuir 15 (1999) 3699.
[5] M. Gopal, W.J. Moberly Chan, L.C. De Jonghe, J. Mater. Sci. 32 (1997) 6001.
[6] K.N.P. Kumer, K. Keizer, A.J. Burggraaf, T. Okubo, H. Nagamoto, S. Morooka, Nature 358 (1992) 48.
[7] S. Ito, S. Inoue, H. Kawada, M. Hara, M. Iwasaki, H. Tada, J. Colloid. Interf. Sci. 216 (1999) 59.
[8] K. Terabe, K. Kato, H. Miyazaki, S. Yamaguchi, A. Imai, Y. Iguchi, J. Mater. Sci. 29 (1994) 1617.
[9] B.E. Yoldas, J. Mater. Sci. 21 (1986) 1087.
[10] K.S. Suslick, Science 247 (1990) 1439.
[11] K.S. Suslick, S.B. Choe, A.A. Cichowlas, M.W. Grinstaff, Nature 353 (1991) 414.
[12] M.M. Mdleleni, T. Hyeon, K.S. Suslick, J. Am. Chem. Soc. 118 (1996) 5492.
[13] H. Zhang, J.F. Banfield, J. Phys. Chem. B 104 (2000) 3481.
[14] M.E. Zorn, D.T. Tompkins, W.A. Zeltner, M.A. Anderson, Appl. Catal. B 23 (1999) 1.
[15] J. Lin, J.C. Yu, D. Lo, S.K. Lam, J. Catal. 183 (1999) 368.
[16] A. Fernandez, G. Lassaletta, V.M. Jimenez, A. Justo, A.R. Gonzalez-Elipe, J.M. Herrmann, H. Tahiri, Y. Ait-Ichou, Appl. Catal. B 7 (1995) 49.
[17] J. Yu, X. Zhao, Q. Zhao, Thin Solid Films 379 (2000) 7.
[18] H.F. Yu, S.M. Wang, J. Non-Cryst. Solids 261 (2000) 260.
[19] W. Huang, X. Tang, Y. Wang, Y. Koltypin, A. Gedanken, Chem. Commun. (2000) 1415.
[20] A. Piscopo, D. Robert, J.V. Weber, J. Photochem. Photobiol. A 139 (2001) 253.
[21] J.C. Yu, J. Yu, W. Ho, L. Zhang, Chem. Commun., (2001) 1942.